Design and Preparation of a Novel Cross-Linkable, High Molecular Weight, and Bio-Based Elastomer by Emulsion Polymerization

ARTICLE *in* MACROMOLECULES · SEPTEMBER 2012

Impact Factor: 5.8 · DOI: 10.1021/ma301183k

8 AUTHORS, INCLUDING:

Jun MA
University of South Australia
97 PUBLICATIONS **1,850** CITATIONS

SEE PROFILE

Macromolecules

Article

pubs.acs.org/Macromolecules

Design and Preparation of a Novel Cross-Linkable, High Molecular Weight, and Bio-Based Elastomer by Emulsion Polymerization

Runguo Wang,[‡] Jun Ma,[§] Xinxin Zhou,[‡] Zhao Wang,[‡] Hailan Kang,[‡] Liqun Zhang,*[,†,‡] Kuo-chih Hua,[⊥] and Joseph Kulig[⊥]

[†]State Key Laboratory of Organic−Inorganic Composites and [‡]Key Laboratory of Beijing City for Preparation and Processing of Novel Polymer Materials, Beijing University of Chemical Technology, 100029 Beijing, P. R. China

[§]School of Advanced Manufacturing and Mechanical Engineering, University of South Australia, SA5095 Australia

[⊥]Goodyear Innovation Center, Goodyear Tire & Rubber Company, D/463D, P.O. Box 531, Akron, Ohio 44309-3531, United States

Supporting Information

ABSTRACT: A novel cross-linkable, high molecular weight poly(diisoamyl itaconate-*co*-isoprene) (PDII) elastomer was prepared by emulsion polymerization based on itaconic acid, isoamyl alcohol, and isoprene. Both persulfate and redox initiators were used for the copolymerization of diisoamyl itaconate and isoprene at different monomer ratios. Redox-initiated PDII has much higher molecular weight but relatively lower yield than the persulfate-initiated one. PDII with a number-average molecular weight of 352 000 and a glass transition temperature of −39.5 °C was obtained when the mass ratio of diisoamyl itaconate to isoprene was 80/20. Diisoamyl itaconate and isoprene reactivity ratios were determined by two conventional linear methods: the Fineman−Ross method and the Kelen−Tüdös method. Molecular dynamics simulation and FTIR were used to study the interaction between silica and PDII macromolecules, and the result showed that hydrogen bonds were formed between silica silanols and PDII macromolecules. Silica-reinforced PDII exhibited good mechanical performance, such as ultimate tensile strength above 11 MPa and elongation at break above 400%.

INTRODUCTION

With extensive interest in sustainable development, the chemical industry is making great attempts to replace petrochemical-based monomers with natural ones.[1,2] It is strategically important to construct new polymers or replace present polymers by renewable resources. With the development of fermentation technology, bio-based polymers, especially bio-based plastics, are developing rapidly. Two of the most promising bio-based plastics—poly(lactic acid) and polyhydroxyalkanoates—have been successfully industrialized on a large scale.[3−5] However, compared with bio-based plastics, few bio-based elastomers, especially those targeted for engineering applications, were produced. We intended to synthesize a novel elastomer, which should possesses high molecular weight, low glass transition temperature (T_g), and comprehensive mechanical properties based on renewable monomers that are produced on a large scale.

Itaconic acid is a promising organic acid that has been categorized as one of the "top 12" building block molecules in advanced biorefineries.[6] Although it was first researched in the 1950s, its fermentation process has not reached maturity until the 1990s, and it is now sold at a price of about US $2/kg (Cultor Food Science & Iwata Chemicals) with a worldwide productivity of over 80 000 tons. The large-scale production and low cost of itaconic acid have provided a great opportunity for the synthesis of polymers based on it. However, itaconic acid cannot homopolymerize because of the presence of allylic hydrogen in the molecules that act as chain transfer agents to terminate the propagation of polymer chains.[7,8] Hence, itaconic acid has been used widely in copolymerization with other monomers by condensation polymerization and radical polymerization.[9−18] But in these cases, itaconic acid was used to modify the matrix, and the mass content of itaconic acid in these polymers was less than 10%.

The diesters of itaconic acid can polymerize through either bulk or emulsion polymerization to produce a series of poly(di-*n*-alkyl itaconate)s with ester chains ranging from methyl to eicosyl.[19] The number-average molecular weights of these polymers range from 50 000 to 120 000. With increase in side-chain length of these polymers, T_g increases first and then decreases as a result of side-chain effect. The local crystallinity,[20] dielectric relaxations,[21] dynamic properties,[22] nanophase-separated regions, and side-chain relaxations[23] of poly(di-*n*-alkyl itaconate)s were investigated. These system and comprehensive studies of Cowie, Arrighi, and McEwen provide great opportunities to fabricate renewable polymers based on

Received: June 11, 2012
Revised: July 30, 2012
Published: August 21, 2012

itaconic acid. However, no research has focused on how to design and synthesize an elastomer from itaconic acid, which must possess sufficiently high molecule weight, low T_g, and cross-linkable groups. In spite of previous studies, it is still not clear (i) how to synthesize high molecular weight polymer from itaconic acid; (ii) whether it is possible to introduce double bonds into these polymers, since double bonds are essential to produce cross-linking for elastomers; and (iii) how to synthesize a polymer of low T_g, which is a prerequisite for low-temperature applications.

In this study, we bring out the strategy to synthesize a high molecular weight and cross-linkable elastomer by emulsion polymerization from itaconic acid, isoamyl alcohol, and isoprene. Isoamyl alcohol was used because of the appropriate side chain length to polymerize a low-T_g polymer. Besides, isoamyl alcohol could be produced by fermentation or by the separation from fusel oil.[24−26] In the fuel industry, ethanol and isoamyl alcohol were regarded as biorenewable oxygenated fuels.[27] Collaboration between Genencor Company and Goodyear Company results in breakthrough technology for bioisoprene. The world's first concept demonstration tire made with bioisoprene has been demonstrated during the United Nations Climate Change Conference in Copenhagen (COP 15) in December 2009. Bio-based isoprene will be made available in the market in 2012 by Genencor Company and in 2015 by Amyris Company.[28,29] Thus, PDII elastomer was prepared based on bio-based itaconic acid, bio-based isoamyl alcohol, and potentially bio-based isoprene. Emulsion polymerization was used because it offers several advantages such as enhanced rates of reaction, high molecular weight of products, mild reaction conditions, and mature formulas.[30−32] Furthermore, its wide acceptance by industry to manufacture styrene butadiene rubber (SBR), acrylic rubber (AR), chloroprene rubber (CR), and nitrile butadiene rubber (NBR) implies a potential readily commercialization for poly(diisoamyl itaconate-*co*-isoprene) elastomers. The results indicated that it is convenience to obtain high molecular weight and low-T_g polymer by redox-initiated polymerization. The synthesized elastomer could be readily processed and cross-linked by the current rubber processing facilities and methods. Through reinforcement by silica, PDII/silica composites exhibit highly improved mechanical performance than neat PDII.

MATERIALS AND METHODS

Materials. Itaconic acid (purity of 99%) was obtained from Shandong Qingdao Langyatai Group Co. Ltd. Isoamyl alcohol (Natural Product, purity of 97%) was purchased from Sigma-Aldrich Company. Isoprene (purity of 95%) was purchased from Alfa Asear Company and distilled to remove stabilizing agent before use. Ferric ethylenediaminetetraacetic acid salt (Fe-EDTA), oleic acid, sodium hydroxymethane sulfinate (SHS), *tert*-butyl hydroperoxide (TBH), potassium phosphate tribasic, potassium chloride, and hydroxylamine were purchased from Sigma-Aldrich Company and used without further purification. All other chemicals are reagent-grade commercial products and are used as received without further purification.

Preparation of Diisoamyl Itaconate Monomer. Into a 1 L three-neck glass flask equipped with a condenser, a thermometer, a mechanical agitator, and a Dean−Stark decanter, 104.1 g of itaconic acid, 282.1 g of isoamyl alcohol, and 31.2 g of cyclohexane were added. After the mixture was heated to 110−115 °C, 0.37 g of sulfuric acid was added as catalyst. As indicated in Scheme 1, the reaction was considered complete when the quantity of byproduct (i.e., water of reaction) reached a theoretical value (27.5 mL). The product was washed by deionized water (DI) in a separating funnel and distilled in vacuum to obtain diisoamyl itaconate.

Scheme 1. Schematic of Diisoamyl Itaconate Synthesis

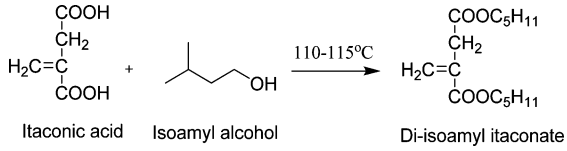

Synthesis of Poly(diisoamyl itaconate-*co*-isoprene) (PDII) by Persulfate-Initiated Emulsion Polymerization. The persulfate-initiated emulsion copolymerization of diisoamyl itaconate and isoprene was carried out using the recipe showed in Table 1. The

Table 1. Recipe for Persulfate-Initiated Emulsion Polymerization

ingredients	amount (g)
diisoamyl itaconate	variable
isoprene	variable
deionized water	250
sodium dodecyl sulfate (SLS)	2.5
polyoxyethylene octylphenol ether (OP-10)	2.5
ammonium persulfate (APS)	0.35
$NaHCO_3$	1.5

reaction system included a 1 L steel reactor equipped with an anchor stirrer running at 350 rpm, a sampling system, a digital thermometer, a pressure detector, and a N_2 inlet. The temperature of the reaction was controlled with a thermostatic bath. The polymerization was carried out as follows: First, the emulsifier, the stabilizer and deionized water were added into the reactor. The temperature was kept below 25 °C because isoprene is volatile, the monomers were loaded, and the pressure was increased to 0.8 MPa. Once the polymerization was started by addition of an aqueous solution of APS, the stirring speed immediately reduced to 250 rpm. Then, the polymerization was allowed to proceed for 20 h to form a stable latex. Obtained by the coagulation of the latex using ethanol, PDII was moved out, washed with deionized water, and dried at 60 °C in vacuum until constant weight. For all PDII, molecular weight, yield, and gel content were determined. The polymerization equation is shown in Scheme 2.

Scheme 2. Schematic of PDII Synthesis

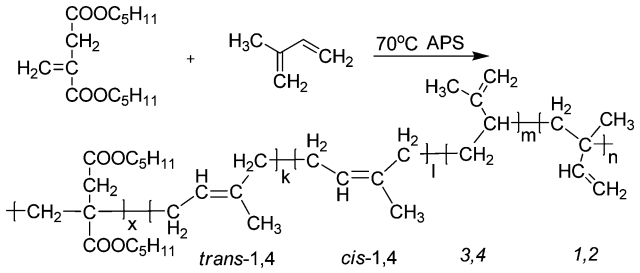

Synthesis of PDII by Redox-Initiated Emulsion Polymerization. The polymerization reactor was a 1 L four-neck glass flask equipped with a reflux condenser, a sampling device, a nitrogen inlet, and a two-bladed anchor-type impeller. According to the recipe in Table 2, DI water, potassium oleate solution, potassium phosphate tribasic solution, and potassium chloride solution were added into the flask under high-speed stirring (450 rpm). Subsequently, diisoamyl itaconate and isoprene were added into the flask, and the stirring speed reduced to 250 rpm. A stable and homogeneous latex was obtained after 30 min stirring. Later, Fe-EDTA solution, SHS solution, and TBH solution were injected into the flask. The polymerization was allowed to proceed at 20 °C for 12 h to form the target PDII latex, followed by adding hydroxylamine solution to terminate the polymerization. The PDII latex was coagulated using an excess of

dx.doi.org/10.1021/ma301183k | *Macromolecules* 2012, 45, 6830−6839

Table 2. Recipe for Redox-Initiated Emulsion Polymerization

ingredients	amount (g)
diisoamyl itaconate	variable
isoprene	variable
deionized water	250
potassium oleate solution (10%)	25
potassium phosphate tribasic solution (10%)	2
potassium chloride (10%)	5
SHS solution (10%)	2
Fe-EDTA solution (10%)	0.4
TBH toluene solution (10%)	0.5
hydroxylamine solution (50%)	0.4

ethanol and dried at 60 °C in vacuum until a constant weight was obtained. For all PDII, molecular weight, yield, and gel content were determined.

Preparation of Cross-Linked PDII and PDII/Silica Composites. The PDII and additives were mixed by a 6 in. two-roll mill according to the formulation given in Table 3. The compound was

Table 3. Compounding Formulation for Cross-Linked PDII and PDII/Silica Composites

ingredients	loading (phr)[a]
PDII	100
silica (Tixosil 383)	variable
zinc oxide	5
stearic acid	0.5
accelerator M[b]	0.7
accelerator CZ[c]	1
sulfur	variable

[a]phr is the abbreviation for weight parts per 100 parts rubber by weight. [b]2-Mercaptobenzothiazole. [c]*N*-Cyclohexyl-2-benzothiazole.

cured in a XLB-D 350 × 350 hot press (Huzhou Eastmachinery Corporation, China) under 15 MPa at 150 °C for its optimum cure time as determined by a disk oscilating rheometer (P3555B2, Beijing Huanfeng Chemical Machinery Experimental Factory, China).

Measurements and Characterization. The FTIR spectra of itaconic acid, diisoamyl itaconate, and PDII were recorded on a Bruker Tensor 27 spectrometer. ^{1}H NMR spectroscopy measurements of diisoamyl itaconate and PDII were carried out with a Bruker AV400 spectrometer. $CDCl_3$ was used as the solvent for the measurements. DSC measurements of PDII were recorded on a Mettler-Toledo differential scanning calorimeter. The samples were heated to 120 °C and maintained for 3 min and then cooled to −80 °C. The heating or cooling rates were 10 °C/min in all cases. The molecular weights of PDII were determined by GPC measurements on a Waters Breeze instrument equipped with three water columns (Styragel HT3_HT5_HT6E) using tetrahydrofuran (THF) as the eluent (1 mL/min) and a Waters 2410 refractive index detector. A polystyrene standard was used for calibration. The gel fractions of PDII were determined by extraction with THF. All samples before testing were extracted in a 2 L glass reactor for 7 h with THF under reflux. After the extraction, these samples were dried, and the gel content was calculated as the ratio of the weight of the dried polymer to its initial weight. The surface morphology of PDII/silica was observed in Hitachi S-4700 scanning electron microscope. An H-800 TEM made by Hitachi, Ltd., in Japan was employed to examine the morphology and distribution of nanoparticles in the PDII/silica. Tensile tests of the silica-filled PDII composites were conducted according to ASTM D412 (dumbbell-shaped) on a LRX Plus tensile tester made by Lloyd Instruments, Ltd., UK.

Calculation of Polymer−Solvent Interaction Parameter χ. In order to estimate the cross-linking density from the equilibrium volume fraction of rubber in the swollen state, the correct evaluation of the Flory−Huggins interaction parameter χ is necessary. The enthalpy of rubber and solvent mixing could be expressed by the Hildebrand semiempirical equation:[33]

$$\Delta H = (n_1 v_1 + n_2 v_2)(\delta_1 - \delta_2)^2 \phi_1 \phi_2 = n_2 v_1 \phi_2 (\delta_1 - \delta_2)^2 \phi_1 \phi_2 \quad (1)$$

where n_1 is the solvent mole number, n_2 is the polymer mole number, v_1 is the solvent mole volume, v_2 is the polymer mole volume, δ_1 is solvent solution parameter, δ_2 is polymer solution parameter, ϕ_1 is volume fraction of solvent in the solution, and ϕ_2 is volume fraction of polymer in the solution.

As the partial mole heat enthalpy ($\Delta\bar{H}$) could be expressed by

$$\Delta\bar{H} = \left(\frac{\partial \Delta H_M}{\partial n_1}\right)_{T,P,n_2} = (\delta_1 - \delta_2)^2 v_1 {\phi_2}^2 \quad (2)$$

The partial mole free energy ($\Delta\bar{G}$) and partial mole entropy ($\Delta\bar{S}$) could be expressed by

$$\Delta\bar{G} = RT\left[\ln(1-\phi_2) + \left(1 - \frac{1}{r}\right)\phi_2 + \chi {\phi_2}^2\right] \quad (3)$$

$$\Delta\bar{S} = -R\left[\ln(1-\phi_2) + \left(1 - \frac{1}{r}\right)\phi_2\right] \quad (4)$$

Based on the equation $\Delta G = \Delta H - T\Delta S$ and eqs 2, 3, and 4, the solvent−polymer interaction parameter χ could be related with δ_1 and δ_2 by

$$\chi = (\delta_1 - \delta_2)^2 v_1 / RT \quad (5)$$

where δ_1 is the solubility parameter of solution and δ_2 is the solubility parameter of polymer.

Calculation of Cross-Linking Density. The PDII vulcanziates with different sulfur contents were swollen in toluene for at total of 72 h. To prepare the samples for weighing, excess solvent on the surfaces of the samples was removed, and then the samples were placed into sealed vials to reduce solvent evaporation during the weighing. At the end of the swelling period, the samples were dried in a vacuum oven at 60 °C for 2 days and weighed again to determine m_d, the mass of the dry network after extraction of soluble materials.

To calculate the cross-linking density of the swollen materials, the Flory−Rehner expression was used. The equation is given as follows:[34,35]

$$v_e = -\frac{\ln(1-v_2) + v_2 + \chi {v_2}^2}{V_s({v_2}^{1/3} - 0.5 v_2)} \quad (6)$$

where v_e is cross-linking density of elastomer, v_2 is the volume fraction of polymer at equilibrium swelling, χ is the polymer−solvent interaction parameter, and v_s is the molar volume of the solvent. The polymer volume fraction follows as

$$v_2 = \left[1 + \left(\frac{m_{eq} - m_d}{m_d}\right)\left(\frac{\rho_2}{\rho_1}\right)\right]^{-1} \quad (7)$$

where ρ_2 and ρ_1 are the densities of the polymer and solvent, respectively, and m_{eq} is the mass of the swollen network at equilibrium.

Molecular Dynamic Simulation. For the molecular dynamic simulation, the Discover and Amorphous Cell modulus of the Materials Studio suite of software were used.[36] All the theoretical calculations were performed by using the condensed-phase optimized molecular potentials for atomistic simulation studies (COMPASS) force field.[37] In this force-field approach, the total energy E_T of the system is represented by the sum of bonding and nonbinding interactions given as

$$E_T = E_b + E_0 + E_\varphi + E_{loop} + E_{pe} + E_{vdw} + E_q \quad (8)$$

dx.doi.org/10.1021/ma301183k | *Macromolecules* 2012, 45, 6830−6839

The first five terms represent the bonding interactions, which correspond to energies associated with the bond E_b, bond angle bending E_θ, torsion angle rotation E_φ, out of loop E_{loop}, and potential energy E_{pe}. The last two terms represent the nonbonding interactions, which consist of the van der Waals term E_{vdw} and electrostatic force E_q. This force-field approach describes the intramolecular and intermolecular interactions in the chemical system of silica filled PDII composite. The COMPASS force field has been widely used to optimize and predict the structural, conformational, and thermophysical condensed phase properties of molecules including polymers. Initial velocities were set by using the Maxwell−Boltzmann profiles at 298 K. The Verlet velocity time integration method[38] was used with the time step of 1 fs.

Amorphous cells were constructed containing blends of four chains of 50 repeat units of PDII and silica. First, the PDII polymer chains and silica were built in periodic boundary cell (Figure 1). Then the cell

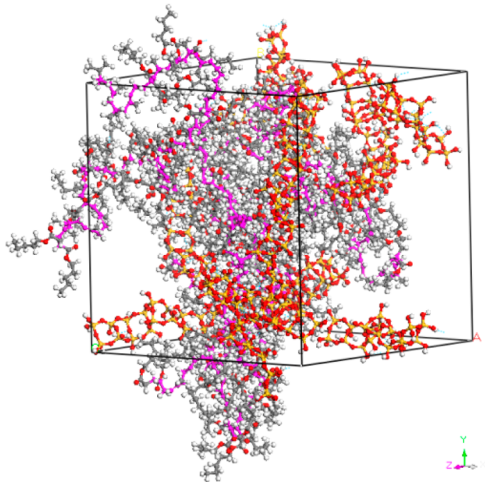

Figure 1. Simulation for hydrogen bonding through molecular modeling using Materials Studio Software (in the unit cell: red, O; white, H; gray, C; yellow, Si; purple, back bonds of PDII matrix).

was taken by energy minimization to get the cell with the lowest energy. After that, the systems were equilibrated in the isothermal−isobaric (NPT) ensemble at 298 K. This equilibration was usually done for 5 ps with the dynamics that was followed by the data accumulation running for at least 100 ps with the configurations saved every 5 ps. At last, the proper cell can be used to analysis hydrogen bonds.

RESULTS AND DISCUSSION

Synthesis and Structure of Diisoamyl Itaconate. Itaconic acid was capped with isoamyl alcohol, a renewable monomer, to restrain the chain transfer effect of carboxyl groups and achieve high molecular weight (Scheme 1). In Figure 2, the resonances at 6.25 and 5.63 ppm are both assigned to the C═CH_2 protons of itaconate, indicative of double bonds for subsequent polymerization. Absorptions at 1.47, 4.07, and 4.14 ppm are due to the *b*, *e*, and *f* protons of the methylenes groups of the capped product, respectively. The absorptions at 1.64 and 0.87 ppm belong to the −CH proton and $-CH_3$ protons of the isoamyl units, respectively. In conclusion, diisoamyl itaconate was produced in this step.

Synthesis of Poly(diisoamyl itaconate-*co*-isoprene) (PDII) by Persulfate-Initiated Emulsion Polymerization. According to the previous studies,[39−42] the polymerizations of itaconates and acrylates are usually initiated by persulfates like ammonium persulfate and potassium persulfate. Thus, persulfate-initiated free radical copolymerization of diisoamyl

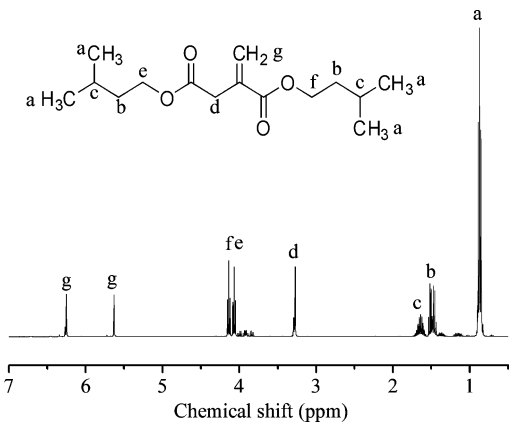

Figure 2. ^{1}H NMR spectrum of diisoamyl itaconate.

itaconate and isoprene was carried out at 70 °C under 0.8 MPa. High temperature is designed to ensure sufficient free radicals for polymerization, and high pressure is designed to keep isoprene as liquid state during the emulsion polymerization. As shown in Table 4, the number-average molecular weight (M_n)

Table 4. Molecular Weight, T_g, Yield, and Gel Content of Persulfate-Initiated PDII

samples	DIA/g	IP/g	M_n	M_w/M_n	T_g/°C	gel/%	yield/%
APS-1	100	0	19 000	2.76	−2.5	0	85.3
APS-2	95	5	23 000	2.70	−8.7	0	83.5
APS-3	90	10	33 000	2.71	−21.3	0	90.2
APS-4	80	20	84 000	3.62	−32.5	1	93.7
APS-5	70	30	74 000	3.98	−39.5	2	85.3
APS-6	60	40	64 000	4.25	−44.5	2	77.5
APS-7	50	50	56 000	4.14	−49.2	3	71.1
APS-8	0	100	49 000	4.26	−57.5	9	59.6

of poly(diisoamyl itaconate) is 19 000, the glass transition temperature (T_g) is −2.5 °C, and the polydispersity index is 2.76. With the increase of isoprene content, M_n of PDII ranges from 23 000 to 84 000. The increase of M_n could be explained as follows: homopolymerization of diisoamyl itaconate retained due to the steric effect of its pendant end groups. However, this steric effect poses little effect during copolymerization wherein diisoamyl itaconate reacts with a low-volume monomer isoprene. Furthermore, the T_g keeps on decreasing as a result of the high flexibility of the isoprene units in PDII. The polydispersity index also increase with the isoprene content because the increase of chain transfer effect increases the number of branch structures. The gel content of PDII increases with isoprene content, which caused by micro-cross-linking between the macromolecular chains due to the existence of double bonds. The yield of the PDII keeps at a high level which ranges from 71.1% to 93.7%.

Synthesis of PDII by Redox-Initiated Emulsion Polymerization. Molecular weight is important for the mechanical properties of polymers. For conventional elastomers, widely used nature rubber (NR), styrene butadiene rubber (SBR), and arcylic rubber (AR) usually have a M_n above 200 000.[43] However, the M_n of persulfate-initiated PDII was below 100 000, much less than conventional elastomers. In order to increase the M_n of PDII, redox-initiated polymerization was carried out at 20 °C under atmospheric pressure. Oxidant sodium hydroxymethane sulfinate and reductant Fe-EDTA

dx.doi.org/10.1021/ma301183k | *Macromolecules* 2012, 45, 6830−6839

were introduced to decrease the activation energy of *tert*-butyl hydroperoxide radical decomposition, assuring sufficient free radicals generated in the polymerization.

In Table 5, the M_n of redox-initiated poly(diisoamyl itaconate) is 55 000, much larger than persulfate-initiated poly(diisoamyl itaconate). The explanation is that redox-initiated polymerization was carried out at low temperature; chain transfer and chain termination effect acted much less than persulfate-initiated polymerization. Therefore, redox-initiated polymerization is more conducive to propagate the macromolecular chains and form high molecular weight polymers. With increase of isoprene content, the M_n ranges from 84 000 to 352 000 and reaches a maximum at 20 wt %. PDII synthesized by redox polymerization has far higher molecular weights than the persulfate-initiated PDII. For example, the M_n of PDII with 20 wt % isoprene is 4-fold increase over the persulfate-initiated PDII with the same isoprene content. The gel content of redox-initiated PDII is larger than persulfate-initiated PDII as micro-cross-linking formed more frequently for redox-initiated PDII due to their large molecular weight. The same as persulfate-initiated PDII, the polydispersity index increases and the T_g keeps on decreasing with the increase of isoprene content. By comparsion, the T_g of redox-initiated PDII is slightly lower than the persulfate-initiated PDII.

Table 5. Molecular Weight, T_g, Yield, and Gel Content of Redox-Initiated PDII

samples	DIA (g)	IP (g)	M_n	M_w/M_n	T_g (°C)	gel (%)	yield (%)
redox-1	100	0	55 000	2.20	−4.2	0	50.3
redox-2	95	5	84 000	3.05	−10.6	1	53.7
redox-3	90	10	142 000	3.28	−25.5	1	55.3
redox-4	80	20	352 000	3.41	−39.5	2	85.7
redox-5	70	30	316 000	3.66	−42.1	2	88.0
redox-6	60	40	256 000	4.12	−48.2	3	71.3
redox-7	50	50	317 000	3.94	−53.8	5	62.2
redox-8	0	100	286 000	4.21	−61.5	17	48.5

NMR and FTIR Characterization of PDII. Emulsion polymerization of isoprene by redox emulsion polymerization was carried on to investigate the composition of PDII. In Figure 3, the sharp signals from methyl proton of cis-1,4 unit (j) and trans-1,4 (d) were observed at 1.68 and 1.58 ppm, respectively. According to previous NMR studies on polyisoprene,[44−49] the peaks above 4.50 ppm indicate olefinic protons of 3,4-addition (4.61−4.78 ppm) and 1,2-addition (5.71−5.78 ppm). It was found that the polyisoprene prepared by redox emulsion polymerization at 20 °C consists of 70.6% of trans-1,4, 19.9% of cis-1,4, 4.5% of 1,2-addition, and 5.0% of 3,4-addition structures.

As shown in Figure 4, the sharp signal at 0.92 ppm corresponds to the $-CH_3$ of the diisoamyl itaconate units.

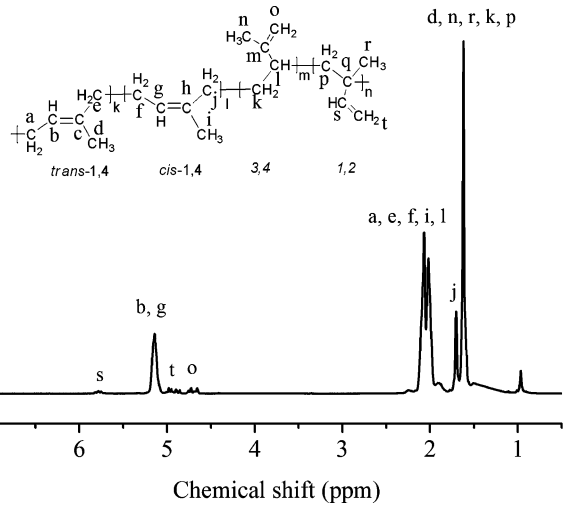

Figure 3. ^{1}H NMR spectrum of redox-initiated polyisoprene.

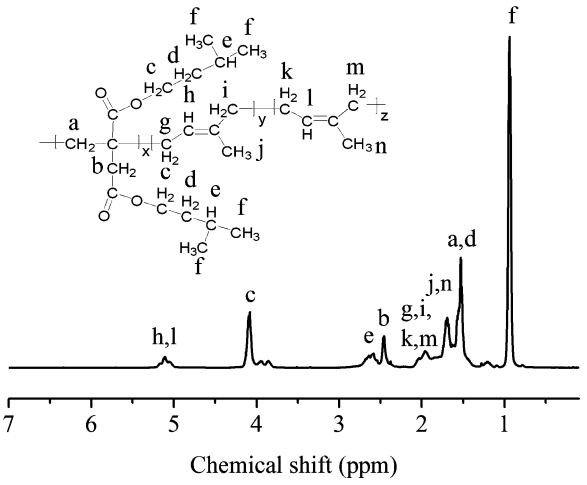

Figure 4. ^{1}H NMR spectrum of PDII with diisomayl itaconate/isoprene mass ratio as 80/20.

Chemical shifts for the protons of 1,2-addtion units and 3,4-addition units were not observed. PDII dominantly consists of trans-1,4 units and cis-1,4 units. The reason was that due to the steric hinerance of diisoamyl itaconate, 1,2-addition, and 3,4-addition were difficult to form.

Figure 5 contains the FTIR spectra of itaconic acid, diisoamyl itaconate, poly(diisoamyl itaconate), and PDII. The intense C═O vibration peak at 1740 cm^{-1} is associated with the formation of ester bonds. In Figure 5b, the presence of double bonds in diisoamyl itaconate can be verified by the absorptions at 1641 and 816 cm^{-1} for the stretching and bending vibrations.

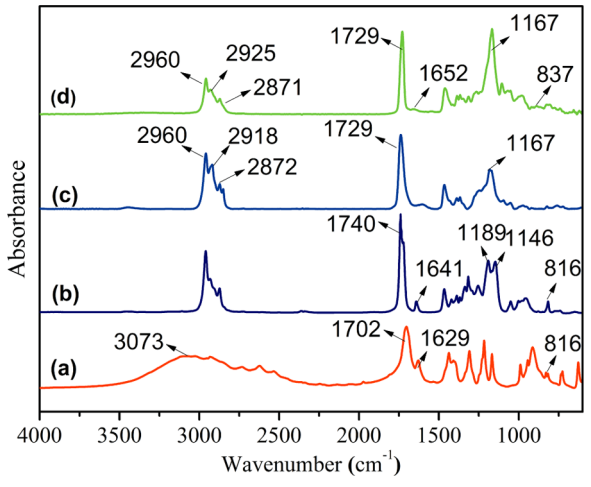

Figure 5. FTIR spectra of (a) itaconic acid, (b) diisoamyl itaconate, (c) poly(diisoamyl itaconate), and (d) PDII with diisoamyl itaconate/isoprene mass ratio of 80/20.

dx.doi.org/10.1021/ma301183k | *Macromolecules* 2012, 45, 6830−6839

The disappearance of both absorptions after homopolymerization and copolymerization confirms the transformation of monomers to polymer. The dual absorption peaks (1189 and 1146 cm^{-1}) of C−O−C for diisoamyl itaconate are due to the existence of double bonds. One of the neighboring −C═O groups is conjugated to the C═C group, but the other is not. After polymerization, the dual absorption peaks transform to a single absorption peak at 1167 cm^{-1}. The broad absorptions at 2960, 2925, and 2871 cm^{-1} are attributed to the stretching vibration of $-CH_3$, $-CH_2$, and −CH in the PDII, respectively. The absorption at 1652 cm^{-1} corresponds to the stretching vibration of C═C, and the absorption at 837 cm^{-1} corresponds to the bending vibration of C−H in the isoprene units. According to ^1H NMR and FTIR results, isoprene has been successfully copolymerized with diisoamyl itaconate.

Thermal Properties of PDII. Thermal properties such as crystallization and glass transition temperatures (T_g) are critical for elastomers because a crystalline or semicrystalline polymer is not elastic. Elastomers should have a T_g lower than room temperature, and an ideal T_g for elastomers should be lower than −30 °C.[50] Nonisothermal DSC results from −70 to 60 °C for a variety of PDII specimens indicate a completely amorphous structure for PDII. In Figure 6, the decrease in T_g with increasing isoprene content is caused by the increase of macromolecular flexibility by the introduction of isoprene units. Copolymers containing more than 10 wt % isoprene show sufficiently low T_g, and these materials should be ideal candidates for elastomers.

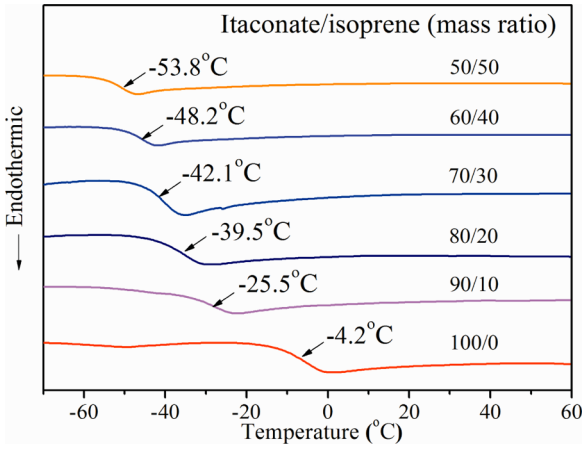

Figure 6. DSC thermograms of redox-initiated PDII with different diisoamyl itaconate/isoprene ratios.

Reactivity Ratios of Diisoamyl Itaconate and Isoprene. The reactivity ratios of diisoamyl itaconate (DIA) and isoprene (IP) in the redox emulsion polymerization were calculated by linearization methods, specifically the Fineman−Ross (FR) method[51] and Kelen−Tüdös (KT) method.[52] The conversion of monomers was controlled to below 10%, as supported by yield calculations. By calculations of areas under the peaks *h*, *l*, and *f*, in the ^1H NMR spectrum in Figure 3, the copolymer composition was determined. The FR and KT parameters for the copolymers are presented in Table 6. The FR plot and KT plot are shown in Figure 7. The correlation coefficients for the FR plot and the KT plot are 0.994 and 0.990, respectively.

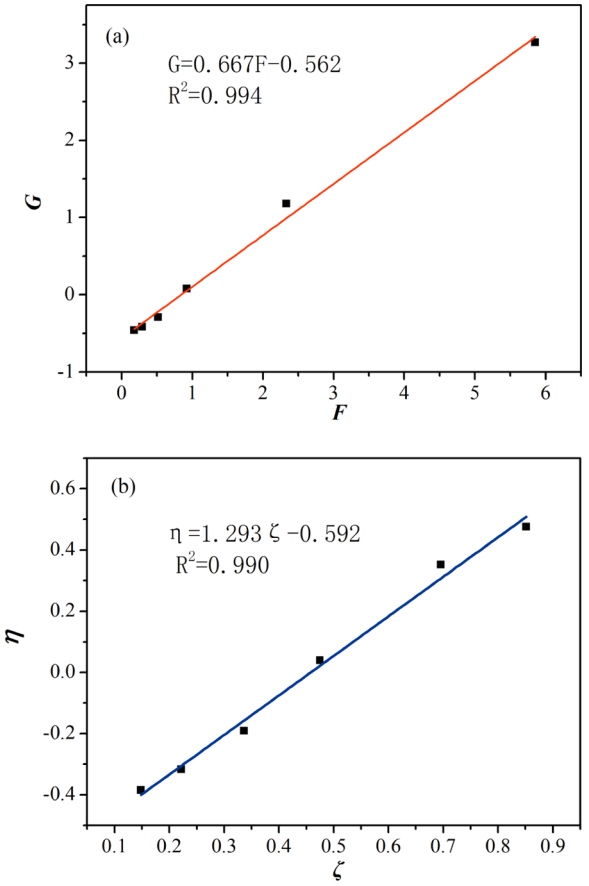

Figure 7. Calculations of reactivity ratios of diisoamyl itaconate and isoprene in redox emulsion copolymerization: (a) Fineman−Ross method and (b) Kelen−Tüdös method.

In Table 7, the r_{DIA} and r_{IP} values obtained from both methods are in good agreement with each other. Since the values of r_{DIA} and r_{IP} are less than one, the copolymerization of DIA and IP belongs to an azeotropic polymerization with an

Table 6. Parameters for Calculation of Reactivity Ratios of Diisoamyl Itaconate and Isoprene[a]

sample	$F = M_1/M_2$	$f = m_1/m_2$	$G = F(f-1)/f$	$H = F^2/f$	$\eta = G/(\alpha + F)$	$\zeta = H/(\alpha + H)$
S1	4.787	3.444	3.397	6.653	0.756	0.858
S2	2.268	2.086	1.181	2.465	0.518	0.692
S3	1.008	1.066	0.063	0.953	0.054	0.465
S4	0.588	0.678	−0.279	0.510	−0.342	0.317
S5	0.378	0.488	−0.396	0.293	−0.566	0.211
S6	0.252	0.351	−0.465	0.181	−0.736	0.141

[a] $\alpha = (H_{max} \times H_{min})^{1/2} = 1.097$, M_1: molar fraction of diisoamyl itaconate in the feed; M_2: molar fraction of isoprene in the feed; m_1: molar fraction of diisoamyl itaconate in the copolymer; m_2: molar fraction of isoprene in the copolymer.

dx.doi.org/10.1021/ma301183k | Macromolecules 2012, 45, 6830−6839

Table 7. Reactivity Ratios of Diisoamyl Itaconate and Isoprene

methods	r_{DIA}	r_{IP}	$r_{DIA} \times r_{IP}$	azeotropic point[a]
Fineman–Ross	0.67	0.56	0.38	0.57
Kelen–Tüdös	0.70	0.60	0.42	0.57
average	0.69	0.58	0.40	0.57

[a]Azeotropic point = $(1 - r_{IP})/(2 - r_{DIA} - r_{IP})$.

azeotropic point 0.57. The polymerization of PDII, if carried out at a DIA molar fraction of 0.57, will produce a copolymer of the same composition as the feed. A molar fraction of DIA less than 0.57 should give a product with a higher fraction of DIA units than feed, and a molar fraction of DIA higher than 0.57 should give a product with a lower fraction of DIA units than that of the feed. Also, the r_{DIA} and r_{IP} values imply that both monomers possess strong alternating capacity and thus can copolymerize well to produce a high molecular weight copolymer than the homopolymer of DIA.

Time Dependence of PDII Synthesis. To investigate the effect of reaction time on the M_n of PDII and the yield of the copolymerization, we carried out the redox emulsion polymerization of PDII at a fixed diisoamyl itaconate/isoprene mass ratio of 80/20. Figure 8 shows that the yield increases with

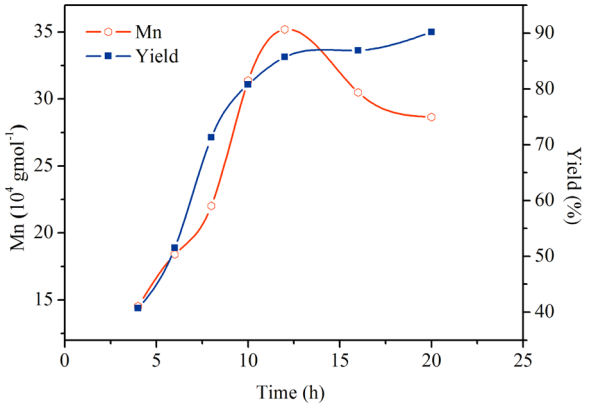

Figure 8. Time dependence of M_n and yield of PDII at diisoamyl itaconate/isoprene mass ratio of 80/20.

reaction time, reaching 90.2% after 20 h; the M_n of PDII increases from 4 to 12 h and then decreases. This decrease would be caused by the oligomers produced, in agreement with previous studies.[53,54] Redox-4 (see Table 5) is picked, which has a diisoamyl itaconate/isoprene mass ratio of 80/20 and gives a copolymer with a M_n of 352 000, polydispersity index of 3.41, and yield of 85.7% at 12 h, for further compounding and curing studies.

Curing Characteristics and Mechanical Properties of PDII. Most elastomer products are useless unless properly cured. Since the modulus of the elastomer increases dramatically during curing, it is used to monitor the curing progress. Figure 9 shows the characteristic curing curves for neat PDII with different sulfur contents at 150 °C. From the typical cure curves, it can be concluded that PDII could be effectively cross-linked by sulfur. Scorch time, cure time, and torque increase of neat PDII vulcanizates are depicted in Table 8. The results show that scorch time and cure time of the vulcanizates decreased, and torque increase of the vulcanizates increased with the increase of sulfur content. The tensile strength increases from 0.49 to 1.34 MPa, but the elongation at

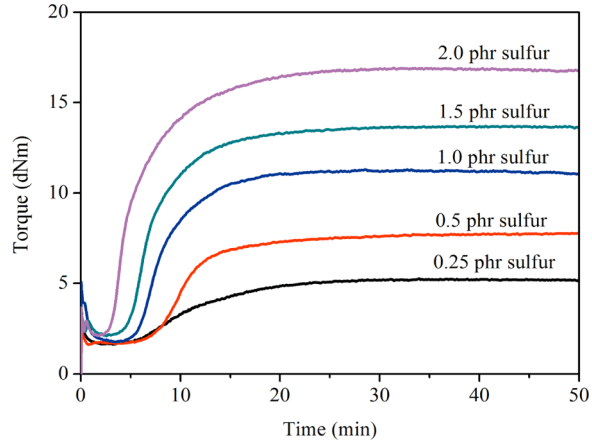

Figure 9. Curing curves of neat PDII with different amounts of sulfur.

Table 8. Curing Parameters of Neat PDII with Different Amounts of Sulfur

	sulfur (phr)	scorch time (min:s)	cure time (min:s)	torque increase (dN m)
(a)	0.25	6:12	20:33	3.64
(b)	0.5	7:30	18:12	6.18
(c)	1.0	5:54	14:33	9.21
(d)	1.5	5:06	13:48	11.62
(e)	2.0	3:35	13:53	14.83

break decreases from 644.1% to 198.9% with the increase of sulfur content, as shown in Figure 10. It is well-known that a

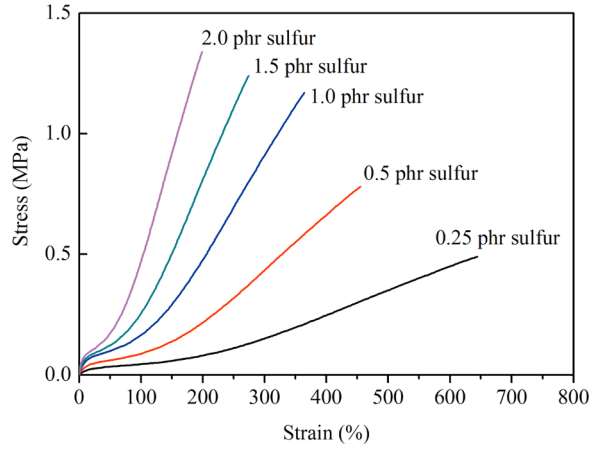

Figure 10. Stress–strain curves of neat PDII with different amounts of sulfur.

higher cross-linking density provides a higher degree of restraining macromolecular disentanglement and decoiling, leading to a higher strength but a lower elongation.[55,56] The result implies that the mechanical properties of PDII could be readily manipulated by adjusting the cross-linking density. In order to give a quantitative control of cross-linking density of PDII vulcanizates, the calculation of cross-linking density was carried out.

Cross-linking density was calculated by the Flory–Rehner expression shown in eq 6. For conventional elastomers, polymer–solvent interaction parameter could be inquired in polymer handbooks. However, polymer–solvent interaction parameter between solvent and PDII needs to be calculated by

dx.doi.org/10.1021/ma301183k | Macromolecules 2012, 45, 6830–6839

the relationship with solubility parameter, as described in eq 5. A method often used to calculate solubility parameter is based on an evaluation of maximum in swelling using a series of solvents of varying and known solubility parameters. The assumption is that the interaction and swelling will be a maximum when the solubility parameter of the polymer matches that of the solvent.[57,58] In Table 9, nine solvents

Table 9. Calculation of Solubility Parameter of PDII

solvents	density (g/cm^3)	δ_s (J/mL)$^{1/2}$	W_0 (g)	W' (g)	Q
n-hexane	0.6594	14.99	0.0535	0.1068	2.4243
n-heptane	0.6836	15.23	0.0576	0.1292	2.7142
cyclohexane	0.7786	16.76	0.0577	0.2410	4.8463
carbon tetrachloride	1.5940	17.58	0.0486	0.5388	6.9652
toluene	0.8669	18.20	0.0665	0.4773	7.7176
chloroform	1.4840	19.85	0.0592	1.1600	12.7487
n-propanol	0.8036	23.25	0.0629	0.1122	1.9195
ethanol	0.8160	26.39	0.0658	0.0748	1.1580
methanol	0.7910	29.67	0.0628	0.0665	1.0702

with different solubility parameters are applied to the calculation of solubility parameter δ. Then we use swelling ratio Q ($V_{solution}/V_{PDII}$) to characterize swelling content. As shown in Figure 11, the solubility parameter δ of PDII is 19.85

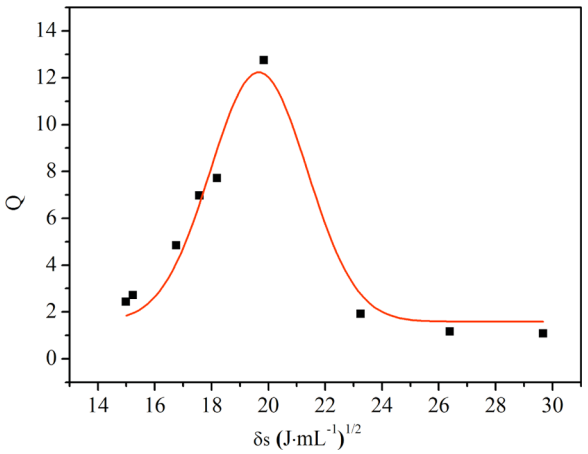

Figure 11. Relationship between swelling ratio and solubility parameter.

(J/mL)$^{1/2}$. From the value of δ, the value of χ can be calculated based on eq 5, and the value is 0.12. Then the cross-linking density could be calculated by eq 6, and the results are listed in Table 10. As expected, cross-linking density of PDII vulcanizates significantly increases with the increase of sulfur content.

Table 10. Cross-Linking Density of PDII Vulcanizates with Different Sulfur Content

sample	sulfur content (phr)	cross-linking density (10^{-5} mol/cm^3)
1	0.25	3.3
2	0.5	5.6
3	1.0	8.8
4	1.5	12.5
5	2.0	18.6

With low tensile strength and amorphous structure, PDII need to be reinforced by fillers. It was compounded with silica nanoparticles toward reinforcement due to two reasons below: (i) As shown in Scheme 2, ester groups exist in the PDII pendent chains. Since numberous silanol groups exist on the surface of silica, we hypothesis these ester groups would interact with silica via hydrogen bonding, leading to a uniform dispersion and thus a desired improvement in mechanical performance. (ii) Silica is independent of petroleum, which would otherwise make the application of PDII reliant on the declining petroleum resource.

Molecular Dynamics Simulation of Hydrogen Bonds (HBs) in PDII/Silica Composites. In order to identify the hydrogen bonding in the PDII/silica composites, the molecular dynamics simulation method was used. In Figure 1, the PDII chains and silica nanoparticles were built in an amorphous cell to calculate the number, length, and angle of the HBs, with the PDII to silica weight mass ratio fixed at 60/40.[59] As shown in Figure 12, the PDII macromolecular chains can form HBs on

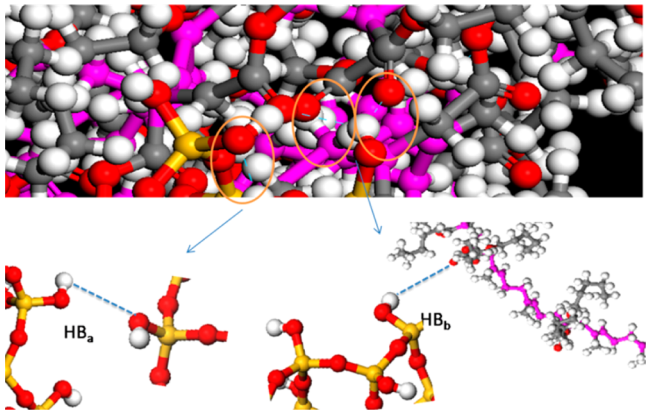

Figure 12. Formation of two types of HBs between silica and PDII matrix simulated by molecular modeling using Material Studio Software.

the silica surface, leading to an improved compatibility between PDII and silica nanoparticles. Two types of HBs are formed in the composites: (i) HB$_a$ formed between the silica nanoparticles and (ii) HB$_b$ formed between the PDII ester groups and the −OH groups on the nanoparticle surface. The second type HBs contribute to the homogeneous dispersion of silica particles in PDII.

Then we investigated the hydrogen bond length in these composites. It is known that the length of a hydrogen bond determines the strength of the bond (Table 11).[60] Figure 13

Table 11. Classification of Strong, Moderate, and Weak Hydrogen Bonds

	strong	moderate	weak
bond lengths [Å] H---A	1.2−1.5	1.5−2.2	>2.2

shows our simulation results of hydrogen bond length versus its angle. Each point in these clusters represents a HB$_b$ which was obtained from the molecular dynamics simulation results. Based on the classification of hydrogen bonds by bond length, the HB$_b$s were mainly scattered in the moderate region.

Following the simulation, FTIR was carried on for the research of HB$_b$. From Figure 14, significant changes in the

dx.doi.org/10.1021/ma301183k | *Macromolecules* 2012, 45, 6830−6839

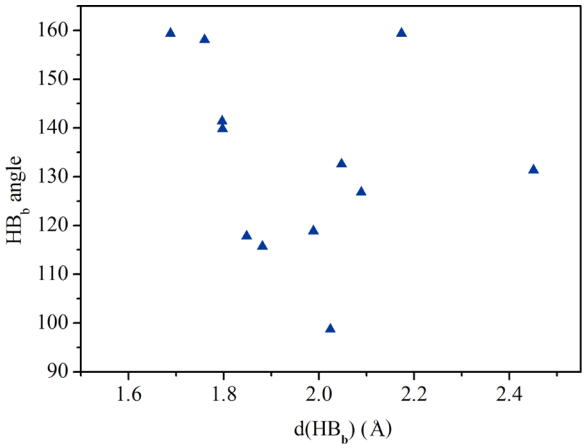

Figure 13. Angular scatter plot of HB_b angles against HB_b distances.

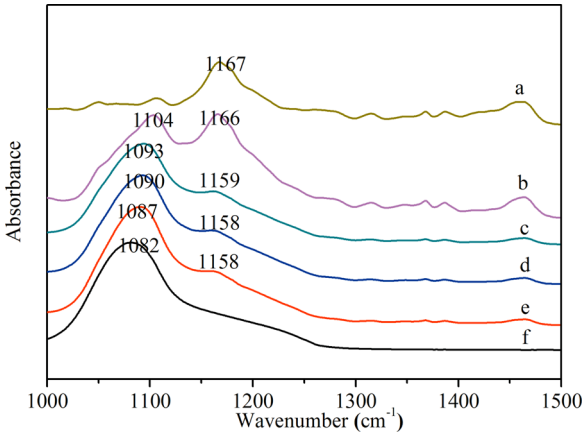

Figure 14. Dependence of silica content on FTIR spectra of the hybrids; the weight ratio of PDII/silica is (a) 100:0, (b) 80:20, (c) 60:40, (d) 40:60, (e) 20:80, and (f) 0:100.

peaks between 1000 and 1500 cm^{-1} in their FTIR spectra were observed for different hybrids. The absorption peak located at 1167 cm^{-1} characteristic of −C═O and C−O−C stretching vibrations in PDII, red-shifted in the hybrids, so did the peak located at 1083 cm^{-1} characteristic of Si−O−Si stretching vibration. These facts indicated that the silanol groups formed HBs with −C═O and C−O−C in the mixtures.

SEM and TEM were used to investigate the morphology of PDII/silica hybrids. Figure 15 shows the morphology of PDII/silica (weight ratio: 60/40) hybrids. The silica particles in the hybrid are in the range 10−30 nm and are dispersed well in the hybrid. This also may caused by the HB_b between organic and inorganic components, which prevented the aggregation of silica particles.

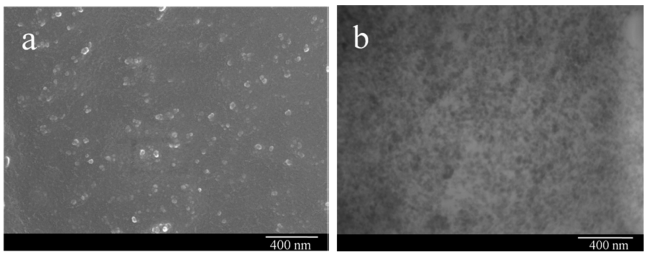

Figure 15. SEM (a) and TEM (b) images of PDII/silica composites.

Mechanical Properties of PDII/Silica Composites. As shown in Figure 16, with the increase of silica content, the

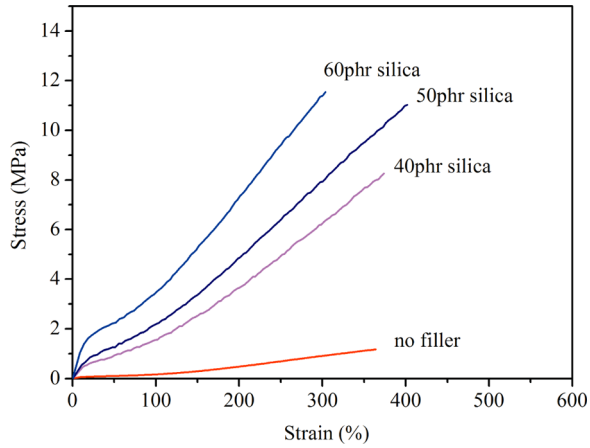

Figure 16. Strain−stress curves of PDII/silica composites.

tensile strength increases significantly, and the elongation at break reaches a maximum at 50 phr and then decreases. With 50 phr silica, the tensile strength of the composite increases to 8.9 times that of the neat PDII, and the elongation at break increases from 364.2% to 413.5%. Even though elastomers could be remarkably reinforced by fillers, but only happens with homogeneous dispersion. The good reinforcement effect of PDII with silica proves good dispersion and strong interfacial interaction between silica and PDII matrix. The silica filled PDII composites may be good candidates for wide applications as low-temperature-resistant and oil-resistant rubber products.

CONCLUSIONS

A high molecular weight and cross-linkable poly(diisoamyl itaconate-*co*-isoprene) (PDII) elastomer was fabricated from itaconic acid, isoamyl alcohol, and isoprene by emulsion polymerization. With isoprene content of 20 wt %, the number-average molecular weight of PDII reached 352 000, and the glass transition temperature was −39.5 °C. The reactivity ratios of both monomers calculated by the Fineman−Ross method and the Kelen−Tüdös method were less than one and in agreement with each other, indicating that (i) the copolymerization is an azeotropic polymerization and (ii) the monomers possess a strong alternating capacity and thus can copolymerize well to produce high molecular weight. According to molecular dynamics simulation and FTIR results, hydrogen bonds exist between PDII macromolecules and silica silanols. The tensile strength of silica-reinforced PDII composite exceeded over 11 MPa and the elongation at break was over 400%, satisfactory performance for some engineering applications.

ASSOCIATED CONTENT

Supporting Information

FTIR data of the characterization of the esterification of itaconic acid and isoamyl alcohol; photos of the persulfate-initiated PDII and the redox-initiated PDII. This material is available free of charge via the Internet at http://pubs.acs.org.

AUTHOR INFORMATION

Corresponding Author

*E-mail: zhanglq@mail.buct.edu.cn.

Notes

The authors declare no competing financial interest.

■ ACKNOWLEDGMENTS

This work was supported by the National Natural Science Foundation of China (50933001), the National Science Foundation for Distinguished Young Scholars of China (50725310), and the National Basic Research Program (973 Program) of China (2011 CB606003). Thanks for the financial support of Goodyear Tire & Rubber Company.

■ REFERENCES

(1) Gandini, A. *Macromolecules* **2008**, *41*, 9491−9504.
(2) Kurian, J. V. *J. Polym. Environ.* **2005**, *13*, 159−167.
(3) Pang, X.; Zhuang, X.; Tang, Z.; Chen, X. *Biotechnol. J.* **2010**, *5*, 1125−1136.
(4) Shen, L.; Worrell, E.; Patel, M. *Biofuels, Bioprod. Biorefin.* **2010**, *4*, 25−40.
(5) Snell, K. D.; Peoples, O. P. *Biofuels, Bioprod. Biorefin.* **2009**, *3*, 456−467.
(6) Orts, W. J.; Holtman, K. M.; Seiber, J. N. *J. Agric. Food Chem.* **2008**, *56*, 3892−3899.
(7) Bartlett, P. D.; Nozaki, K. *J. Polym. Sci.* **1948**, *3*, 216−222.
(8) Bartlett, P. D.; Altschul, R. *J. Am. Chem. Soc.* **1945**, *67*, 816−822.
(9) Ni, H.; Kawaguchi, H.; Endo, T. *Macromolecules* **2007**, *40*, 6370−6376.
(10) Meaurio, E.; Velada, J. L.; Cesteros, L. C.; Katime, I. *Macromolecules* **1996**, *29*, 4598−4604.
(11) Liu, G.; Ding, X.; Cao, Y.; Zheng, Z.; Peng, Y. *Macromolecules* **2004**, *37*, 2228−2232.
(12) Landry, C. J. T.; Coltrain, B. K.; Teegarden, D. M.; Ferrar, W. T. *Macromolecules* **1993**, *26*, 5543−5551.
(13) Barrett, D. G.; Merkel, T. J.; Luft, J. C.; Yousaf, M. N. *Macromolecules* **2010**, *43*, 9660−9667.
(14) Aguiar, A.; González-Villegas, S.; Rabelero, M.; Mendizábal, E.; Puig, J. E.; Domínguez, J. M.; Katime, I. *Macromolecules* **1999**, *32*, 6767−6771.
(15) Krusic, M. K.; Filipovic, J. *Polymer* **2006**, *47*, 148−155.
(16) Willke, T.; Vorlop, K. D. *Appl. Microbiol. Biotechnol.* **2001**, *56*, 289−295.
(17) Erbil, C.; Yildiz, Y.; Uyanik, N. *Polym. Adv. Technol.* **2009**, *20*, 926−933.
(18) Oliveira, M. P.; Giordani, D. S.; Santos, A. M. *Eur. Polym. J.* **2006**, *42*, 1196−1205.
(19) Cowie, J. M. G.; Henshall, S. A. E.; McEwen, I. J.; Velickovic, J. *Polymer* **1977**, *18*, 612−616.
(20) Arrighi, V.; Triolo, A.; McEwen, I. J.; Holmes, P.; Triolo, R.; Amenitsch, H. *Macromolecules* **2000**, *33*, 4989−4991.
(21) Arrighi, V.; McEwen, I. J.; Holmes, P. F. *Macromolecules* **2004**, *37*, 6210−6218.
(22) Arrighi, V.; Holmes, P. F.; Gagliardi, S.; McEwen, Q.; Telling, M. T. F. *Appl. Phys. A: Mater. Sci. Process.* **2002**, *74*, S466−S468.
(23) Arrighi, V.; Holmes, P. F.; McEwen, I. J.; Terrill, N. J.; Qian, H. *J. Mater. Chem.* **2004**, *14*, 3306−3307.
(24) Bandres, M.; de Caro, P.; Thiebaud-Roux, S.; Borredon, M.-E. *C. R. Chim.* **2011**, *14*, 636−646.
(25) Piang-Siong, W.; de Caro, P.; Lacaze-Dufaure, C.; Shum Cheong Sing, A.; Hoareau, W. *Ind. Corp. Prod.* **2012**, *35*, 203−210.
(26) Fortman, J. L.; Chhabra, S.; Mukhopadhyay, A.; Chou, H.; Lee, T. S.; Steen, E.; Keasling, J. D. *Trends Biotechnol.* **2008**, *26*, 375−381.
(27) Cataluna, R.; da Silva, R.; de Menezes, E.; Ivanov, R. *Fuel.* **2008**, *87*, 3362−3368.
(28) Singh, R. *Org. Process Res. Dev.* **2010**, *15*, 175−179.
(29) Yang, J.; Zhao, G.; Sun, Y.; Zheng, Y.; Jiang, X.; Liu, W.; Xian, M. *Bioresour. Technol.* **2012**, *104*, 642−647.
(30) Blackley, D. C. *High Polymer Latices: Their Science and Technology*; Palmerton Publishing Co. Inc.: New York, 1966.
(31) El-Aasser, M.; Lovell, P. *Emulsion Polymerization and Emulsion Polymers*; John Wiley & Sons, Inc.: Chichester, 1997.
(32) Gilbert, R. G. *Emulsion Polymerization: A Mechanistic Approach*; Academic Press: London, 1995.
(33) Orwoll, R. A. *Rubber Chem. Technol.* **1977**, *50*, 451−479.
(34) Flory, P. J.; Rehner, J. J. *J. Chem. Phys.* **1943**, *11*, 512−520.
(35) Flory, P. J.; Rehner, J. J. *J. Chem. Phys.* **1943**, *11*, 521−526.
(36) Peng, F.; Pan, F.; Sun, H.; Lu, L.; Jiang, Z. *J. Membr. Sci.* **2007**, *300*, 13−19.
(37) Sun, H. *J. Phys. Chem. B* **1998**, *102*, 7338−7364.
(38) Khalili, M.; Liwo, A.; Rakowski, F.; Grochowski, P.; Scheraga, H. A. *J. Phys. Chem. B* **2005**, *109*, 13785−13797.
(39) Plessis, C.; Arzamendi, G.; Leiza, J. R.; Alberdi, J. M.; Schoonbrood, H. A. S.; Charmot, D.; Asua, J. M. *J. Polym. Sci., Polym. Chem.* **2001**, *39*, 1106−1119.
(40) Capek, I.; Potisk, P. *Eur. Polym. J.* **1995**, *31*, 1269−1277.
(41) Otsu, T.; Watanabe, H. *Eur. Polym. J.* **1993**, *29*, 167−174.
(42) Carrillo, M.; de Ilarduya, A. M.; Arnal, M. L.; Torres, C.; Lopez-Carrasquero, F. *Polym. Bull.* **2002**, *48*, 59−66.
(43) Mark, J. E. *Polymer Data Handbook*; Oxford University Press: New York, 1999.
(44) Cheong, I. W.; Fellows, C. M.; Gilbert, R. G. *Polymer* **2004**, *45*, 769−781.
(45) Stoffelbach, F.; Tibiletti, L.; Rieger, J.; Charleux, B. *Macromolecules* **2008**, *41*, 7850−7856.
(46) Cataldo, F.; Ragni, P.; Rosati, A.; Ursini, O. *Radiat. Phys. Chem.* **2009**, *78*, 338−344.
(47) Zhang, J.; Xue, Z. *Polym. Test.* **2011**, *30*, 753−759.
(48) Kostjuk, S. V.; Ouardad, S.; Peruch, F.; Deffieux, A.; Absalon, C.; Puskas, J. E.; Ganachaud, F. *Macromolecules* **2011**, *44*, 1372−1384.
(49) Bonnet, F.; Visseaux, M.; Pereira, A.; Barbier-Baudry, D. *Macromolecules* **2005**, *38*, 3162−3169.
(50) Hofmann, W. *Rubber Technology Handbook*; Hanser Publishers: Munich, 1989.
(51) Fineman, M.; Ross, S. D. *J. Polym. Sci.* **1950**, *5*, 259−262.
(52) Kelen, T.; Tüdös, F. *J. Macromol. Sci., Chem.* **1975**, *A9*, 1−27.
(53) Sarac, A. S. *Prog. Polym. Sci.* **1999**, *24*, 1149−1204.
(54) Lamb, D. J.; Fellows, C. M.; Gilbert, R. G. *Polymer* **2005**, *46*, 7874−7895.
(55) Zosel, A.; Ley, G. *Macromolecules* **1993**, *26*, 2222−2227.
(56) Bokern, S.; Fan, Z.; Mattheis, C.; Greiner, A.; Agarwal, S. *Macromolecules* **2011**, *44*, 5036−5042.
(57) Yagi, Y.; Inomata, H.; Saito, S. *Macromolecules* **1992**, *25*, 2997−2998.
(58) Elif Hamurcu, E.; Baysal, B. M. *J. Polym. Sci., Polym. Phys.* **1994**, *32*, 591−594.
(59) Qiao, B.; Zhao, X. Y.; Yue, D. M.; Zhang, L. Q.; Wu, S. Z. *J. Mater. Chem.* **2012**, *22*, 12339−12348.
(60) Karimi-Varzaneh, H. A.; Carbone, P.; Müller-Plathe, F. *Macromolecules* **2008**, *41*, 7211−7218.